JACS
JOURNAL OF THE AMERICAN CHEMICAL SOCIETY

Communication

pubs.acs.org/JACS

Hydrazone Switch-Based Negative Feedback Loop

Susnata Pramanik and Ivan Aprahamian*

Department of Chemistry, Dartmouth College, Hanover, New Hampshire 03755, United States

Supporting Information

ABSTRACT: A negative feedback loop that relies on the coordination-coupled deprotonation (CCD) of a hydrazone switch has been developed. Above a particular threshold of zinc(II), CCD releases enough protons to the environment to trigger a cascade of reactions that yield an imine. This imine sequesters the excess of zinc(II) from the hydrazone switch, hence lowering the effective amount of protons, and switching the cascade reactions "OFF", thus establishing the negative feedback loop.

Feedback loops are involved in the control of various processes ranging from climate and computing systems to the stock market.[1] Such loops are also crucial in biology because they ensure homeostasis by regulating sugar concentration, blood pressure and body temperature, among other processes.[2] Glycogenesis, for example, is triggered when glucose levels rise above a certain threshold. This process triggers a complex signaling cascade that initiates the release of insulin followed by glycogen synthesis, which leads to the lowering of blood glucose concentration to an optimal level.[3] This example is an instance of a negative feedback loop. In positive feedback loops, on the other hand, the product of a reaction amplifies the process that causes its production. Although the latter is common in synthetic organic systems (e.g., autocatalysis),[4] there has been an appreciable lag in the development of negative feedback loops. Whereas artificial biological components have been exploited to demonstrate negative feedback mechanisms,[5] chemical-based negative loops have not been explored beyond a small number of oscillating reactions.[6] The development of negative feedback loops based on synthetic organic compounds, although not trivial, is important for the design of processes, such as oscillating systems, which are governed by nonequilibrium thermodynamics. More importantly, they are crucial in imparting adaptivity[7] to chemically fueled dissipative systems (e.g., out-of-equilibrium self-assemblies) which, although not common,[8] are getting more attention from numerous research communities.[9]

We[10] and others[11] have been interested in developing multicomponent switching[12] and signaling cascades[13] as a means of mimicking the complexity[14] of biological systems. For this systems chemistry[15] approach to be successful, different types of self-regulating mechanisms must be established, particularly ones that can function as negative feedback loops. Herein, we report such a process utilizing coordination-coupled deprotonation (CCD).[16] The system works as follows (Scheme 1): below a certain level of zinc(II) concentration (depicted with a black equilibrium arrow) CCD does not produce enough protons to catalyze the deprotection of compound **3**. Once the threshold is exceeded (depicted with red arrows), the protons begin to catalyze the deprotection, leading to aminoquinoline (**4**). Amine **4** and pyridine carbaldehyde (**5**), already present in the solution, combine together and form a thermodynamically more stable bishomoleptic imine complex **6** following the sequestration of zinc(II) from **2** and the remediation of hydrazone **1**. This event lowers in turn the effective concentration of protons in the solution and shuts down the production of the imine complex. This sequence of events was shown to work as a negative feedback loop in which the concentration of zinc(II) is lowered every time it rises above a certain threshold.[17]

Scheme 1. Coordination-Coupled Deprotonation-Initiated Negative Feedback Loop[a]

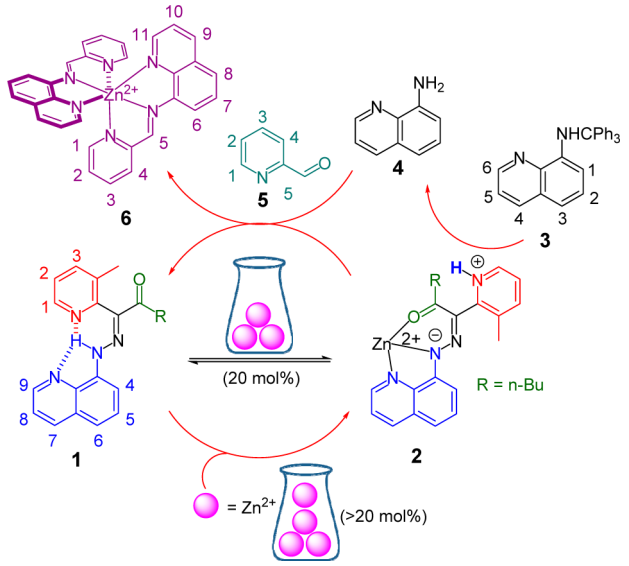

[a]The red arrows depict the process that takes place upon surpassing the threshold amount of zinc(II). The methyltritylether produced with **4** is not shown for the sake of clarity.

We previously found that the CCD prompted release of protons to the environment is optimized in hydrazone switches whose pyridyl ring cannot be coplanar with the rest of the molecule.[13a] Therefore, we decided to incorporate a methylpyridyl ring within the rotor part of compound **1**. Additionally, we introduced a ketone instead of an ester group in the rotor part to reduce the zinc(II) binding affinity of the switch. The targeted hydrazone was synthesized in 65% yield via the

Received: October 7, 2016
Published: November 7, 2016

DOI: 10.1021/jacs.6b10542
J. Am. Chem. Soc. 2016, 138, 15142−15145

condensation reaction between 1-(3-methylpyridin-2-yl)hexan-2-one and quinoline diazonium salt under basic conditions (see Supporting Information). The switch was fully characterized using ^{1}H and ^{13}C NMR spectroscopies, high-resolution mass spectrometry and X-ray crystallography.

The ^{1}H NMR spectrum of **1** in CD_3CN shows the presence of predominantly (>98%) a single isomer in solution (Figure 1a

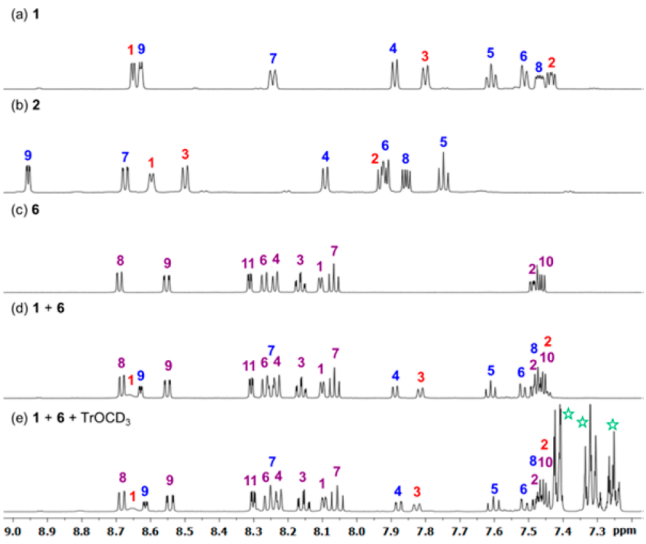

Figure 1. Partial ^{1}H NMR (600 MHz, CD_3CN, 294 K) spectra of (a) the *E*-isomer of hydrazone **1** (a small amount of the *Z*-isomer can also be seen); (b) zinc-bound hydrazone **2**. The spectrum was obtained after reacting **1** with two equivalents of $Zn(ClO_4)_2$ (a small amount of deprotonated zinc-bound complex, $\mathbf{2}_{dp}$, can also be seen); (c) imine complex **6** synthesized separately; (d) hydrazone **1**, and complex **6** (the spectrum was recorded after the addition of 1.0 equiv of $Zn(ClO_4)_2$ to **1** followed by the addition of **4** and **5**, 2 equiv of each); and (e) a mixture of free hydrazone **1**, imine complex **6** and methyltritylether-d_3 (Ph_3COCD_3) (the spectrum was observed when **2** was treated with protected amine **3** and pyridine 2-carbaldehyde (**5**); signals assigned with a green star belong to the Ph_3COCD_3). CD_3OD was employed as cosolvent to capture the liberated trityl cation.

and Figure S1 in the Supporting Information). The hydrazone NH signal appears at 10.7 ppm, which is relatively upfield shifted compared to the previously reported hydrazone systems (13−15 ppm).[18] This chemical shift is attributed to the weak hydrogen bonding between the pyridyl nitrogen and NH proton, which is in accordance with the noncoplanarity of the methylpyridyl ring with the rest of the hydrazone molecule. This assertion is corroborated by the X-ray crystal analysis of **1** (Figure S40 in the Supporting Information). The configuration of **1** was also confirmed by nuclear Overhauser enhancement spectroscopy (NOESY), which shows cross peaks between the butyl protons and proton 4, clearly confirming that the *E*-configuration is the predominant isomer in solution (Figure S5 in the Supporting Information).

The coordination of **1** with $Zn(ClO_4)_2$ is evident by the naked eye as the color of the solution changes from pale yellow to red. Hence, UV−vis spectroscopy was used to calculate the binding affinity of **1** to Zn(II) ($\log K = 4.75 \pm 0.11$, Figures S27 and S28 in the Supporting Information). This process was also probed using ^{1}H NMR spectroscopy (Figure 1b and Figure S12 in the Supporting Information), which showed the disappearance of the hydrazone NH proton upon coordination, indicating the occurrence of CCD. Coordination also leads to *E*/*Z* isomerization, which was confirmed by comparing the changes in the chemical shifts of the quinonyl and pyridyl protons upon coordination (Figure S15 in the Supporting Information), with previously studied systems, and X-ray crystallography (Figure S40 in the Supporting Information). Based on the ^{1}H NMR studies, the outcome of CCD is the formation (>90%) of the zinc-bound, protonated and switched complex **2**, in addition to a minor deprotonated zinc-bound complex ($\mathbf{2}_{dp}$). The identity of the deprotonated complex was established separately using a control experiment in which **2** was treated with base (*N*,*N*-dimethylaminopyridine, DMAP). The obtained spectrum (Figure S16 in the Supporting Information) exactly matches the minor signals observed in the solution mixture.

Next, we utilized the acidic proton of complex **2** to deprotect the aminoquinoline **3** (synthesis and characterization shown in Supporting Information). The catalysis was monitored using ^{1}H NMR spectroscopy and its rate was determined to be 3.03 M^{-1} s^{-1} (Figures S34−S36 in the Supporting Information). To establish that the protons, and not zinc(II), are catalyzing the deprotection, we conducted a control experiment. Compound **2** was deprotonated using DMAP and then **3** was introduced to the mixture. As expected, no deprotection was observed (Figure S21 in the Supporting Information). This experiment clearly demonstrates that the proton released through CCD is responsible for the uncaging of **3**.

To ensure that translocation of zinc(II) occurs from **2** to the newly formed imine compound, we synthesized complex **6** in the presence of **1** (Figure 1d). The addition of 8-aminoquinoline (**4**) and pyridine 2-carbaldehyde (**5**) to an in situ formed complex **2**, led to the formation of **1** and **6** (see Supporting Information for synthesis and characterization) (Figure 1d). The binding affinity of **6** with zinc(II) ($\log K = 9.54 \pm 0.56$; Figure S30 in the Supporting Information) was found to be much larger than that of **1**, which explains why the sequestration takes place.

Subsequently, we studied the deprotection of amine **3** using CCD, by adding **3** and aldehyde **5** to a reaction mixture containing **2**. Encouragingly, we observed that the reaction leads to the free hydrazone **1**, in addition to the formation of the bishomoleptic imine complex **6** with an overall rate of 1.01 M^{-1} s^{-1} (Figure 1e and Figures S37−S39 in the Supporting Information). This same reaction was also carried out in one pot, leading to similar results. Addition of $Zn(ClO_4)_2$ to a mixture of **1**, **3** and **5** (Figure S19 in the Supporting Information) changes the color of the solution from pale yellow to red, indicating the formation of **2**. The color then slowly changes to yellow, as **1** reforms in solution.

These findings prompted us to investigate as to whether we can use the sequence of reactions described above to develop a negative feedback loop. To accomplish this goal, we needed to find a concentration threshold where CCD driven process produces enough protons that can deprotect **3**. Once this happens, **6** will be formed thus sequestering the excess of zinc(II) out of the system, until it falls below the threshold concentration, thus finalizing the negative feedback loop.

We used a mixture of **1** (2.3×10^{-4} M), **2** and **3** (1:2:2) and titrated the solution with small aliquots of $Zn(ClO_4)_2$, and based on the measured reaction rates, waited for 1 h for the system to equilibrate. The ^{1}H NMR spectra (Figure 2) show no formation of imine complex **6** up to 20 (±1) mol % of $Zn(ClO_4)_2$ (Figure 2b); however, when the concentration of $Zn(ClO_4)_2$ is increased about this value, for example to 25 mol

DOI: 10.1021/jacs.6b10542
J. Am. Chem. Soc. 2016, 138, 15142−15145

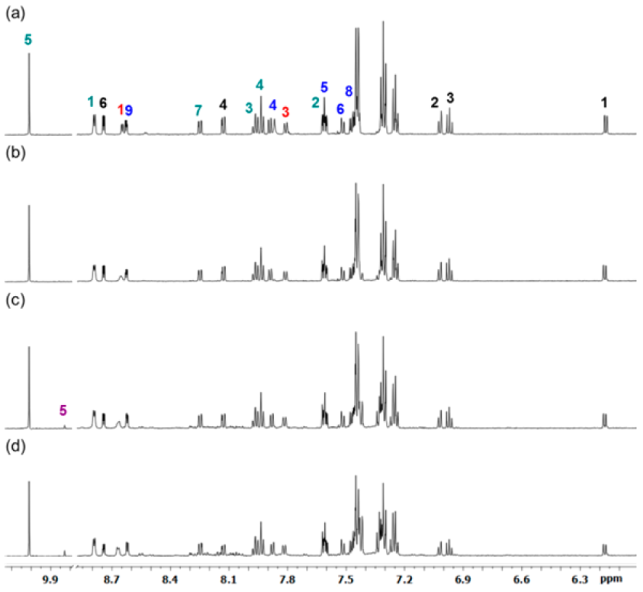

Figure 2. ^{1}H NMR (600 MHz, CD_3CN and CD_3OD (30:1), 294 K) spectra after the addition of (a) 5 mol % of $Zn(ClO_4)_2$ to a mixture of **1**, **3** and **5** (1:2:2). No formation of imine complex **6** is observed; (b) 20 mol % of the $Zn(ClO_4)_2$ to the mixture; (c) 25 mol %, in total, of $Zn(ClO_4)_2$ to the latter mixture. Complex **6** starts forming; and (d) 35 mol % in total of $Zn(ClO_4)_2$ shows incremental formation of **6**.

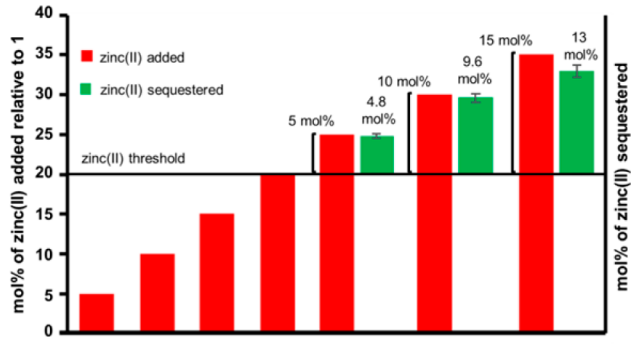

Figure 3. Incremental addition of zinc(II) to a mixture of **1**, **3** and **5** results in the formation of **6**, only after a certain threshold (20 mol %) is passed. The yield of **6** at **25**, **30** and **35** mol % of zinc(II) was measured using ^{1}H NMR spectroscopy, and was found to track well (green bars) with the excess zinc(II) added to the mixture.

%, **6** starts to form (Figure 2c). More importantly, the ^{1}H NMR spectrum after the addition of 25 mol % of the zinc(II) and equilibration for 1 h, reveals that the yield of **6** (6.8×10^{-6} mol) tracks well with the amount of excess metal ions added (7.0×10^{-6} mol) beyond the 20 mol % (Figure 3).[19] This experiment clearly shows that the imine complex formed through CCD is sequestering zinc(II) from **2**, until a certain threshold of zinc(II) is reached, i.e., the negative feedback loop is working.[20]

The fact that the reaction occurs using incremental substoichiometric amounts of $Zn(ClO_4)_2$ (Figure 2d) allowed us to show an "ON/OFF" process in which the reaction that forms **6** proceeds as long as zinc(II) is added to the mixture. When this condition is not satisfied, the solution will contain excess protected amine **3** and aldehyde **5**, in addition to **1** and **6**. Only the addition of stoichiometric amount of $Zn(ClO_4)_2$ will lead to the complete consumption of compounds **3** and **5**. This process is evident in the ^{1}H NMR studies that show the gradual production of complex **6**, upon the addition of 30, 60 and 90 mol %, of $Zn(ClO_4)_2$ relative to **1** (Figure S26 in the Supporting Information).

We have shown that coordination-coupled deprotonation in a hydrazone-based system can be used in devising a negative feedback loop that sequesters zinc(II) from the environment until its concentration falls below a certain threshold. The crucial factors that ensure the function of this system are the (a) release of proton from the hydrazone receptor after zinc(II) binding; and (b) high thermodynamic stability of the newly formed imine complex (**6**) relative to the hydrazone (**2**). We envision that the proper coupling of this negative feedback mechanism with known positive feedback loops will lead to adaptive dissipative assemblies, and new oscillating systems,[6] which will in turn allow us to better understand nonequilibrium processes.

■ ASSOCIATED CONTENT

Supporting Information

The Supporting Information is available free of charge on the ACS Publications website at DOI: 10.1021/jacs.6b10542.

General methods, experimental procedures, NMR spectra of key compounds, kinetic studies (PDF)
Crystallographic data for **2** (CIF)
Crystallographic data for **1** (CIF)

■ AUTHOR INFORMATION

Corresponding Author

*ivan.aprahamian@dartmouth.edu

ORCID

Ivan Aprahamian: 0000-0003-2399-8208

Notes

The authors declare no competing financial interest.

■ ACKNOWLEDGMENTS

We acknowledge the support of the National Science Foundation CAREER program (CHE-1253385). We gratefully acknowledge Prof. Richard Staples (Michigan State University) for X-ray data.

■ REFERENCES

(1) Åström, K. J.; Murray, R. M. Princeton University Press, 2010.
(2) (a) Guyton, A. C.; Hall, J. E.*Textbook of Medical Physiology*; 11th ed.; Elsevier Inc., 2000. (b) Cannon, W. B. *Physiol. Rev.* **1929**, *9*, 399.
(3) Chan, O.; Sherwin, R. S. *Diabetes* **2012**, *61*, 564.
(4) (a) Soai, K.; Shibata, T.; Morioka, H.; Choji, K. *Nature* **1995**, *378*, 767. (b) Szalai, M. L.; Kevwitch, R. M.; McGrath, D. V. *J. Am. Chem. Soc.* **2003**, *125*, 15688. (c) Baker, M. S.; Phillips, S. T. *J. Am. Chem. Soc.* **2011**, *133*, 5170.
(5) (a) Starr, R.; Willson, T. A.; Viney, E. M.; Murray, L. J. L.; Rayner, J. R.; Jenkins, B. J.; Gonda, T. J.; Alexander, W. S.; Metcalf, D.; Nicola, N. A.; Hilton, D. J. *Nature* **1997**, *387*, 917. (b) Naka, T.; Narazaki, M.; Hirata, M.; Matsumoto, T.; Minamoto, S.; Aono, A.; Nishimoto, N.; Kajita, T.; Taga, T.; Yoshizaki, K.; Akira, S.; Kishimoto, T. *Nature* **1997**, *387*, 924. (c) Wasserman, J. D.; Freeman, M. *Cell* **1998**, *95*, 355. (d) Freeman, M. *Nature* **2000**, *408*, 313.
(6) (a) Bray, W. C. *J. Am. Chem. Soc.* **1921**, *43*, 1262. (b) Zhabotinskii, A. M. *Doklady Akademii Nauk SSSR* **1964**, *157*, 392. (c) Briggs, T. S.; Rauscher, W. C. *J. Chem. Educ.* **1973**, *50*, 496. (d) Kovacs, K.; McIlwaine, R. E.; Scott, S. K.; Taylor, A. F. *J. Phys. Chem. A* **2007**, *111*, 549. (e) Poros, E.; Horváth, V.; Kurin-Csörgei, K.; Epstein, I. R.; Orbán, M. *J. Am. Chem. Soc.* **2011**, *133*, 7174. (f) He, X.; Aizenberg, M.; Kuksenok, O.; Zarzar, L. D.; Shastri, A.; Balazs, A. C.;

DOI: 10.1021/jacs.6b10542
J. Am. Chem. Soc. 2016, 138, 15142−15145

Aizenberg, J. *Nature* **2012**, *487*, 214. (g) Orbán, M.; Kurin-Csörgei, K.; Epstein, I. R. *Acc. Chem. Res.* **2015**, *48*, 593. (h) Semenov, S. N.; Kraft, L. J.; Ainla, A.; Zhao, M.; Baghbanzadeh, M.; Campbell, V. E.; Kang, K.; Fox, J. M.; Whitesides, G. M. *Nature* **2016**, *537*, 656.

(7) Grzybowski, B. A.; Wilmer, C. E.; Kim, J.; Browne, K. P.; Bishop, K. J. M. *Soft Matter* **2009**, *5*, 1110.

(8) (a) Boekhoven, J.; Brizard, A. M.; Kowlgi, K. N. K.; Koper, G. J. M.; Eelkema, R.; van Esch, J. H. *Angew. Chem., Int. Ed.* **2010**, *49*, 4825. (b) Korevaar, P. A.; George, S. J.; Markvoort, A. J.; Smulders, M. M. J.; Hilbers, P. A. J.; Schenning, A. P. H. J.; De Greef, T. F. A.; Meijer, E. W. *Nature* **2012**, *481*, 492. (c) Mattia, E.; Otto, S. *Nat. Nanotechnol.* **2015**, *10*, 111. (d) Wood, C. S.; Browne, C.; Wood, D. M.; Nitschke, J. R. *ACS Cent. Sci.* **2015**, *1*, 504. (e) Boekhoven, J.; Hendriksen, W. E.; Koper, G. J. M.; Eelkema, R.; van Esch, J. H. *Science* **2015**, *349*, 1075. (f) Cheng, C.; McGonigal, P. R.; Stoddart, J. F.; Astumian, R. D. *ACS Nano* **2015**, *9*, 8672.

(9) (a) Nédélec, F. J.; Surrey, T.; Maggs, A. C.; Leibler, S. *Nature* **1997**, *389*, 305. (b) Grzybowski, B. A.; Stone, H. A.; Whitesides, G. M. *Nature* **2000**, *405*, 1033. (c) Klajn, R.; Bishop, K. J. M.; Grzybowski, B. A. *Proc. Natl. Acad. Sci. U. S. A.* **2007**, *104*, 10305. (d) Kudernac, T.; Ruangsupapichat, N.; Parschau, M.; Maciá, B.; Katsonis, N.; Harutyunyan, S. R.; Ernst, K. − H.; Feringa, B. L. *Nature* **2011**, *479*, 208. (e) Hermans, T. M.; Frauenrath, H.; Stellacci, F. *Science* **2013**, *341*, 243. (f) Debnath, S.; Roy, S.; Ulijn, R. V. *J. Am. Chem. Soc.* **2013**, *135*, 16789. (g) Weitz, M.; Kim, J.; Kapsner, K.; Winfree, E.; Franco, E.; Simmel, F. C. *Nat. Chem.* **2014**, *6*, 295. (h) Keber, F. C.; Loiseau, E.; Sanchez, T.; DeCamp, S. J.; Giomi, L.; Bowick, M. J.; Marchetti, M. C.; Dogic, Z.; Bausch, A. R. *Science* **2014**, *345*, 1135. (i) Ragazzon, G.; Baroncini, M.; Silvi, S.; Venturi, M.; Credi, A. *Nat. Nanotechnol.* **2015**, *10*, 70. (j) Semenov, S. N.; Wong, A. S. Y.; van der Made, R. M.; Postma, S. G. J.; Groen, J.; van Roekel, H. W. H.; de Greef, T. F. A.; Huck, W. T. S. *Nat. Chem.* **2015**, *7*, 160. (k) Cheng, C.; McGonigal, P. R.; Schneebeli, S. T.; Li, H.; Vermeulen, N. A.; Ke, C.; Stoddart, J. F. *Nat. Nanotechnol.* **2015**, *10*, 547. (l) Zhao, H.; Sen, S.; Udayabhaskararao, T.; Sawczyk, M.; Kučanda, K.; Manna, D.; Kundu, P. K.; Lee, J.-W.; Král, P.; Klajn, R. *Nat. Nanotechnol.* **2016**, *11*, 82.

(10) (a) Su, X.; Aprahamian, I. *Chem. Soc. Rev.* **2014**, *43*, 1963. (b) Tatum, L.; Su, X.; Aprahamian, I. *Acc. Chem. Res.* **2014**, *47*, 2141.

(11) (a) Lehn, J.-M. *Chem. - Eur. J.* **2000**, *6*, 2097. (b) Campbell, V. E.; de Hatten, X.; Delsuc, N.; Kauffmann, B.; Huc, I.; Nitschke, J. R. *Nat. Chem.* **2010**, *2*, 684.

(12) Erbas-Cakmak, S.; Leigh, D. A.; McTernan, C. T.; Nussbaumer, A. L. *Chem. Rev.* **2015**, *115*, 10081.

(13) (a) Ray, D.; Foy, J. T.; Hughes, R. P.; Aprahamian, I. *Nat. Chem.* **2012**, *4*, 757. (b) Pramanik, S.; De, S.; Schmittel, M. *Angew. Chem., Int. Ed.* **2014**, *53*, 4709. (c) Tatum, L.; Foy, J. T.; Aprahamian, I. *J. Am. Chem. Soc.* **2014**, *136*, 17438. (d) Foy, J. T.; Ray, D.; Aprahamian, I. *Chem. Sci.* **2015**, *6*, 209. (e) Ren, Y.; You, L. *J. Am. Chem. Soc.* **2015**, *137*, 14220.

(14) Whitesides, G. M.; Ismagilov, R. F. *Science* **1999**, *284*, 89.

(15) Nitschke, J. R. *Nature* **2009**, *462*, 736.

(16) Su, X.; Robbins, T. F.; Aprahamian, I. *Angew. Chem., Int. Ed.* **2011**, *50*, 1841.

(17) It should be noted that in the absence of hydrazone **1**, zinc(II) will catalyze the deprotection of **3** and lead to the formation of the imine complex **6**. This process will sequester *all* of the zinc(II) from the solution and result in product inhibition. This scenario will be akin to removing all of the glucose from the body during glycogenesis, which is not the aim of a negative feedback loop. The presence of hydrazone **1** ensures that a threshold is established, the catalyst (protons) is never consumed, and zinc(II) is never completely removed from the solution. Hence, hydrazone **1** is crucial for establishing the negative feedback loop.

(18) (a) Landge, S. M.; Aprahamian, I. *J. Am. Chem. Soc.* **2009**, *131*, 18269. (b) Landge, S. M.; Tkatchouk, E.; Benítez, D.; Lanfranchi, D. A.; Elhabiri, M.; Goddard, W. A., III; Aprahamian, I. *J. Am. Chem. Soc.* **2011**, *133*, 9812.

(19) The amount of **6** does not change even after 24h showing that the reaction is indeed turned off (Figure S24 in the Supporting Information).

(20) Based on the calculated binding constant there is not enough free zinc(II) in solution to catalyze the deprotection of **3** (Figure S22 and S25 in the Supporting Information). This confirms that the protons are responsible for the cascade of reactions leading to the imine complex.

DOI: 10.1021/jacs.6b10542
J. Am. Chem. Soc. 2016, 138, 15142−15145